

## ON THE REYNOLDS NUMBER ROLE IN STRUCTURE OF RECIRCULATION ZONE BEHIND BACKWARD FACING STEP IN A NARROW CHANNEL

Václav Uruba

Institute of Thermomechanics, ASCR, v.v.i., Praha

### Abstract

*Topology of the time-mean flow-field behind the backward facing step in a narrow channel is presented for various Reynolds numbers. The flow-field is studied in planes close to the channel bottom and in the plane of symmetry. Special attention is devoted to the appearance of secondary and higher order structures defined on the time-mean basis. Experimental results are obtained from PIV measurements.*

### Introduction

A backward facing step configuration occurs in many practical situations both in nature and in many technical applications in mechanical and civil engineering. Flow separation on the step edge is a source of pressure loss, vibrations, and noise and affects possible heat transfer in the separation zone.

This flow belongs to the complex-flow family defined in the pioneering paper by Bradshaw [1]. The flow over a backward facing step is a very simple as to its geometry but the flow structure is extremely complex both in space and time. The 2D version of flow behind backward facing step has been established as a benchmark configuration for separated flow studies in fluid mechanics. However, fully 3D case related to the flow in a narrow channel is not treated in the available relevant literature adequately.

The flow-field in the recirculation region behind a step in narrow channel is described in [6]. The flow visualization on the channel bottom just behind the step showed a kidney-shaped region, suggesting existence of secondary vortices impinging perpendicularly to the bottom – see Fig. 1.

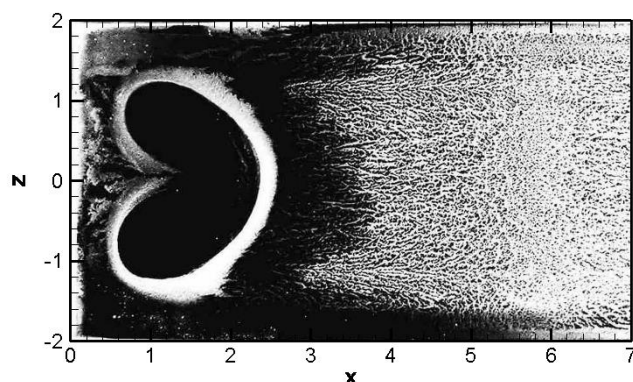


**Fig. 1** Wall visualization on the channel bottom.

The kidney pattern showed up just behind the step, and then back-flow region is located with distinct influence of secondary structures close to the channel walls. The reattachment process could be located in the region for  $x \in (5.5, 6.2)$  close to the channel axis. Reynolds number based on the step height was 34 400, the geometry the same as for the experiments presented below.

The case has been studied in more details. The first publications [2,4] cover especially the mean flow structure, those results have been summarized in [5]. Then, the dynamical behaviour of the flow-field is studied in details. Some aspects of velocity field dynamical behaviour have been addressed in [3]. These introductory studies relied on PIV measurement using stereo system in planes perpendicular to the mean flow. This method showed not very good resolution, especially close to the walls.

The presented paper summarizes new experimental results obtained using classical 2D PIV system acquiring only in-plane velocity components in a measuring plane. Furthermore, the Reynolds number of the flow has been changed in wide range.

## Experimental setup and measuring technique

The existing blow-down test rig was modified for experiments with the separated flow in a channel with a backward facing step. The tunnel has rectangular cross-section with filled corners within the contraction (to suppress corner vortices in the channel entrance), honeycomb and a system of damping screens followed by contraction with contraction ratio 16. The area of the test section input is 0.25 m in height and 0.1 m in width. The time mean velocity departures from homogeneity in planes perpendicular to the tunnel axis are of order tenth of per cent with the exception of corners, where corner vortex starters could be detected. Conventional thickness of boundary layer at the step tip was approximately 2-4 mm depending on velocity. The natural turbulence level was about 0.1 % in the working section input. The channel downstream the backward facing step was 1 m in length. The step itself was 25 mm in height, so the ratio of the input channel width to the step height was 4. All lengths are non-dimensioned using the step height.

The time-resolved PIV method was used for the experiments. The measuring system DANTEC consists of a double-pulse laser with cylindrical optics and CCD camera. The software Dynamics Studio 3.4 was used for velocity-fields evaluation. Laser New Wave Pegasus Nd:YLF, double head, wavelength 527 nm, maximal frequency 10 kHz, a shot energy is 10 mJ for 1 kHz (corresponding power 10 W per head). Camera Phantom V711 has maximal resolution 1280 x 800 pixels and corresponding maximal frequency 3000 double-snaps per second. For the presented measurements the frequency 100 Hz and 2000 double-snaps in sequence corresponding to 20 s of record for evaluation of the mean flow-field. Measurements with higher acquisition frequency have been performed in the same time to capture the flow dynamics. These results are to be presented in future.

The inspected geometry is shown schematically in Fig. 2. Blue colour area is part of channel inlet section, step is grey. The Cartesian coordinate system is introduced with its origin in the middle of the step edge,  $x$ - streamwise direction,  $z$ - spanwise direction and  $y$ - perpendicular to the bottom.

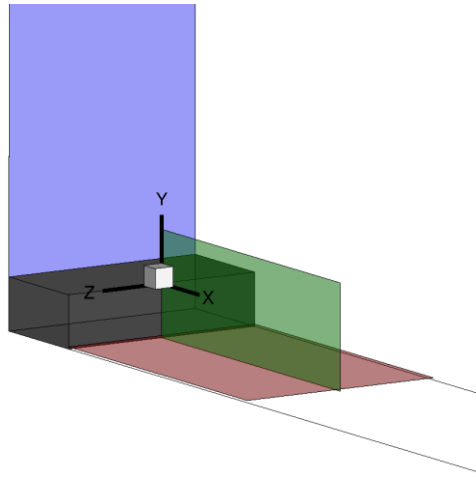


**Fig. 2** Schema of the experiment.

Two types of results are to be presented. The first was acquired in the measuring plane parallel to the channel bottom, about 1.5 mm above it (5 % of the step height). In Fig. 2 the measuring plane is shown in red,  $x \in (0, 6)$ ,  $y = -0.95$  and  $z \in (-2, 2)$ .

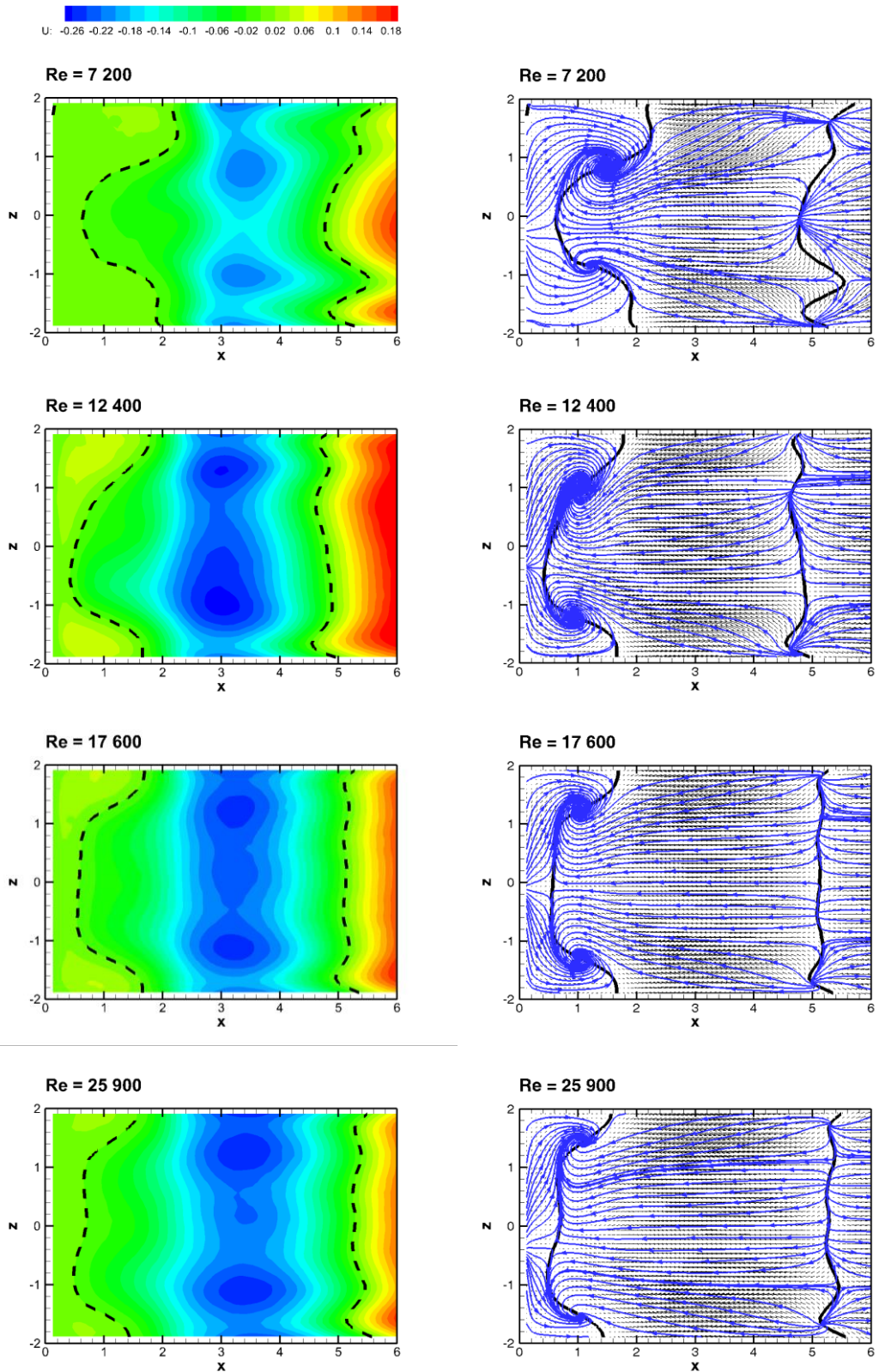
The other measurements have been acquired within the green plane forming the channel plane of symmetry  $x \in (0, 6)$ ,  $y \in (-1, 0.1)$  and  $z = 0$ .

The inflow velocity of air was changed from 4.5 m/s to 20 m/s. The Reynolds number is defined using the inlet velocity, step height and air viscosity, covering range from 7 200 up to 34 400.

## Results

The velocities are scaled by the inlet velocity, so the values are nondimensional and could be compared across the Reynolds numbers. The coordinates are nondimensionalized using the step height.

First, distributions of velocities in the measuring plane parallel to the channel bottom are to be shown. In Fig. 3 the mean streamwise velocity component  $U$  distribution on the left-hand side and velocity vector field  $(U, V)$  on the right-hand side for the Reynolds numbers 7 200, 12 400, 17 600, 25 900 and 34 400. The black line (full and dashed) indicates position of zero streamwise velocity component. To make the vector fields more clear, vector-lines are added in blue in arbitrary way.



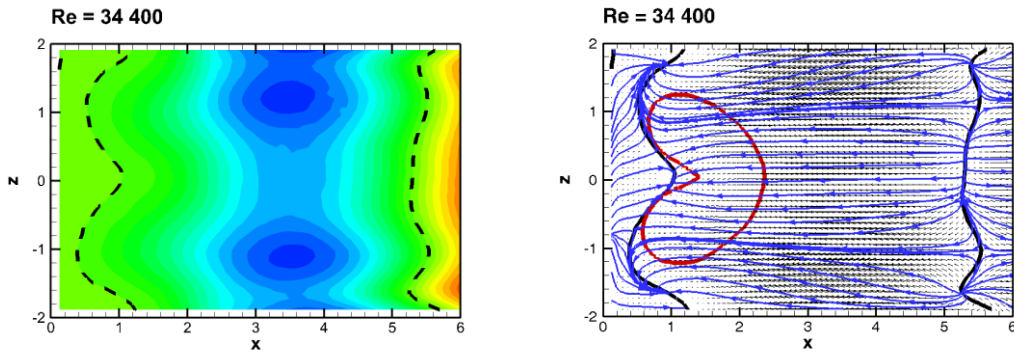


**Fig. 3** Mean streamwise velocity component distribution (left) and velocity vector field (right).  
 Reynolds numbers 7 200, 12 400, 17 600, 25 900 and 34 400.

In Fig. 3 the black lines representing position of vanishing streamwise mean velocity component  $U$ , divide the bottom area into parts with forward ( $U > 0$ ) and backward ( $U < 0$ ) mean flow. Note that between the black lines in the middle of figure the back-flow region is located. Furthermore, for the case  $Re = 34\,400$ , which corresponds to the case studied in [6] shown in Fig. 1, the contour of the kidney structure is added in red.

The velocity distributions in Fig. 3 should be axially symmetrical (axis  $z=0$ ) by definition. Apparently, the symmetry is not perfect. This effect is resulting from imperfections in the channel geometry and/or inflow distribution. The symmetry is better for higher Reynolds numbers.

The two streamwise velocity minima (read back-flow velocity maxima) are located in the centres of each channel half  $z = \pm 1$ , streamwise position starts on  $x = 3$  for low Reynolds numbers and the final position for  $Re = 34\,400$  is about  $x = 3.5$ .

The reattachment region is characterized by the zero streamwise velocity curve in the  $x$  position about 5. It is necessary to note that this is not a real reattachment position, as the velocities are evaluated in the plane a little bit above the wall (about 1.5 mm). The real reattachment region, i.e. the line of zero mean skin friction, is shifted towards the higher  $x$  position. The reattachment line, surprisingly, differs only slightly from the constant  $x$  value across the channel and thus it is close to the 2D situation, however the velocity field within the recirculation zone is highly 3D. The position of reattachment starts on  $x = 5$  for  $Re = 7\,200$  showing important perturbations close to the walls. With raising Reynolds number the line moves in streamwise direction ending on  $x = 5.5$  for  $Re = 34\,400$ . Note that position of reattachment evaluated from wall visualisation in the same case was about  $x = 5.8$  (compare with Fig. 1).

The zero mean streamwise velocity component line just behind the step is highly curved with the closest part about 0.5 downstream the step while the close to the wall it is located in  $x$  position about 1.5-2. The closest point from the step is just in the channel middle  $z = 0$  for small Reynolds numbers, while for Reynolds numbers 25 900 and higher it forms two maxima at  $z = \pm 1$ . For the case of Reynolds number 34 400 this line fits well with the respective kidney shape in the visualisation – see Fig. 4.

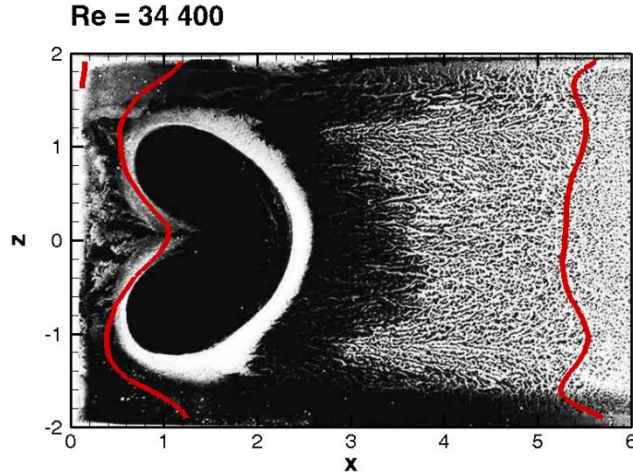


**Fig. 4** Wall visualization on the channel bottom with  $U = 0$  lines.

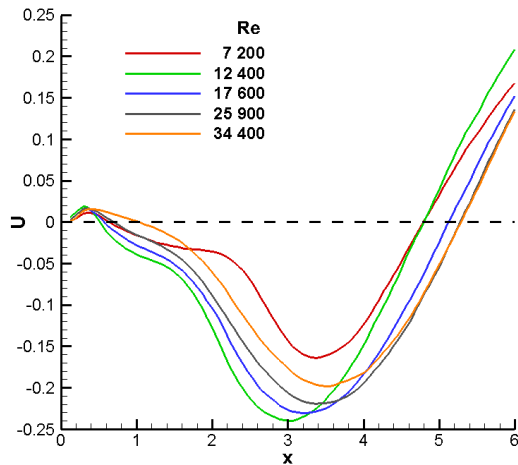
The kidney-shaped region upstream edge follows the line of vanishing streamwise mean velocity component, slight discrepancy could be explained by the fact, that the  $U = 0$  line is evaluated in a certain distance above the bottom.

Furthermore, in the vector-fields (left part of the Fig. 3) another type of secondary structures appear represented by a couple of contra-rotating spirals could be detected with axes perpendicular to the wall with centres moving from the position close to the channel centre towards the walls – see Tab. 1. The spirals could be vortices, but on the time mean basis only, instantaneous topologies are very different from this time mean structure, involving a big number of vortical structures. This issue is to be addressed in a separate presentation dealing with the flow dynamics.

**Tab. 1** Positions of spirals centers just behind the step.

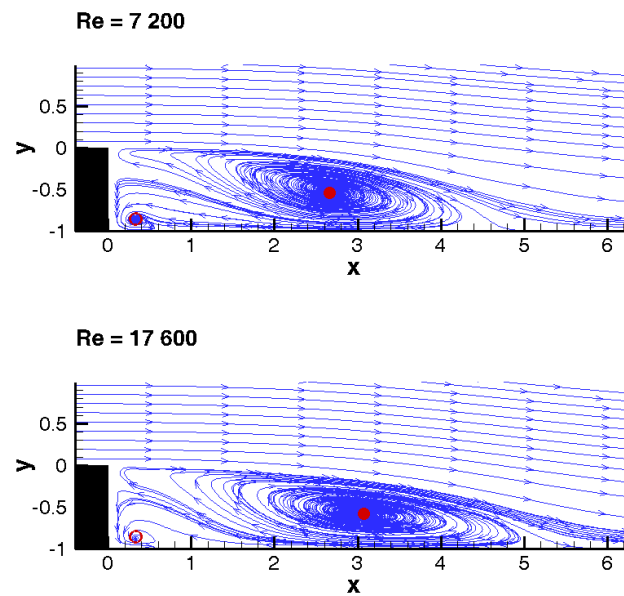
Reynolds number	$x$	$z$
7 200	1.5	$\pm 0.8$
12 400	1	$\pm 1$
17 600	1	$\pm 1.3$
25 900	1	$\pm 1.5$
34 400	0.8	$\pm 1.7$

Comparison of  $U$  velocity component evolution on the  $x$  axis in the measuring plane is shown in Fig. 5 for all Reynolds numbers in question. Size of recirculation zone could be compared easily.



**Fig. 5** Mean streamwise velocity component in  $z = 0$ .

The back-flow between the  $U = 0$  lines in Fig. 3 is connected with a large secondary structure formed by a big spiral, while forward flow direction close to the step for  $0 < x < 1$  is connected with appearance the tertiary vortex. The situation is illustrated in Fig. 6, where the vector lines in the plane of symmetry  $z = 0$  is shown for the three Reynolds numbers 7 200, 17 600 and 34 400 respectively.



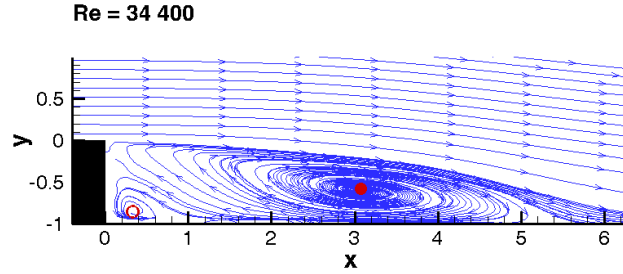
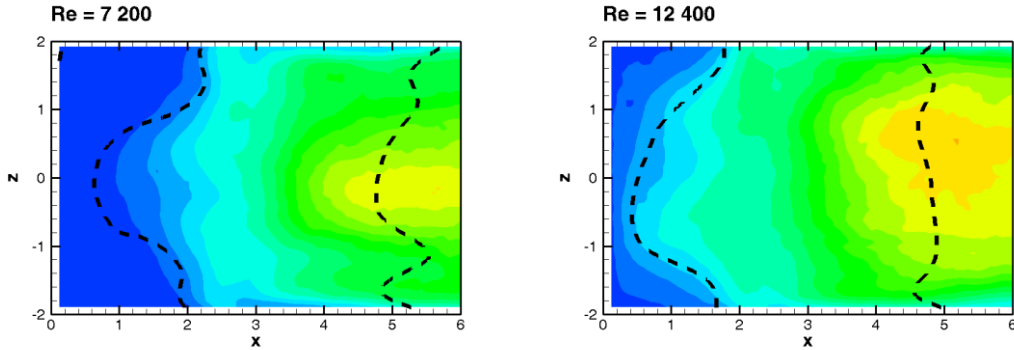


**Fig. 6** Vectorlines in the plane of symmetry.  
Reynolds numbers 7 200, 17 600 and 34 400.

The full red point indicates position of the main secondary recirculation vortex with negative (clockwise) orientation, the hollow point locates the tertiary vortex with positive orientation. The secondary vortex with the center in half step height is moving in downstream direction with increasing Reynolds number from  $x = 2.7$  for  $Re = 7\,200$  to  $x = 3.1$  for  $Re = 34\,400$ . The tertiary vortex is sitting close to both channel bottom and step, on coordinates  $x = 0.3$ ,  $y = 0.1$ .

Note: the lines in Figures represent vector-lines of the time-mean velocity vector field and have incidentally no connection with streamlines or trajectories, which are both based on instantaneous vector fields.

Next, the fluctuation activity has been studied in the plane of measurement. As we have evaluated only in-plane velocity components  $u$  and  $w$  in directions of  $x$  and  $z$  axes respectively, in Fig. 7 the sums of variances of those velocity components are to be shown. The velocities are normalized by the inlet velocity, so the distributions for various Reynolds numbers could be compared directly not only on qualitative basis, but also quantitatively.



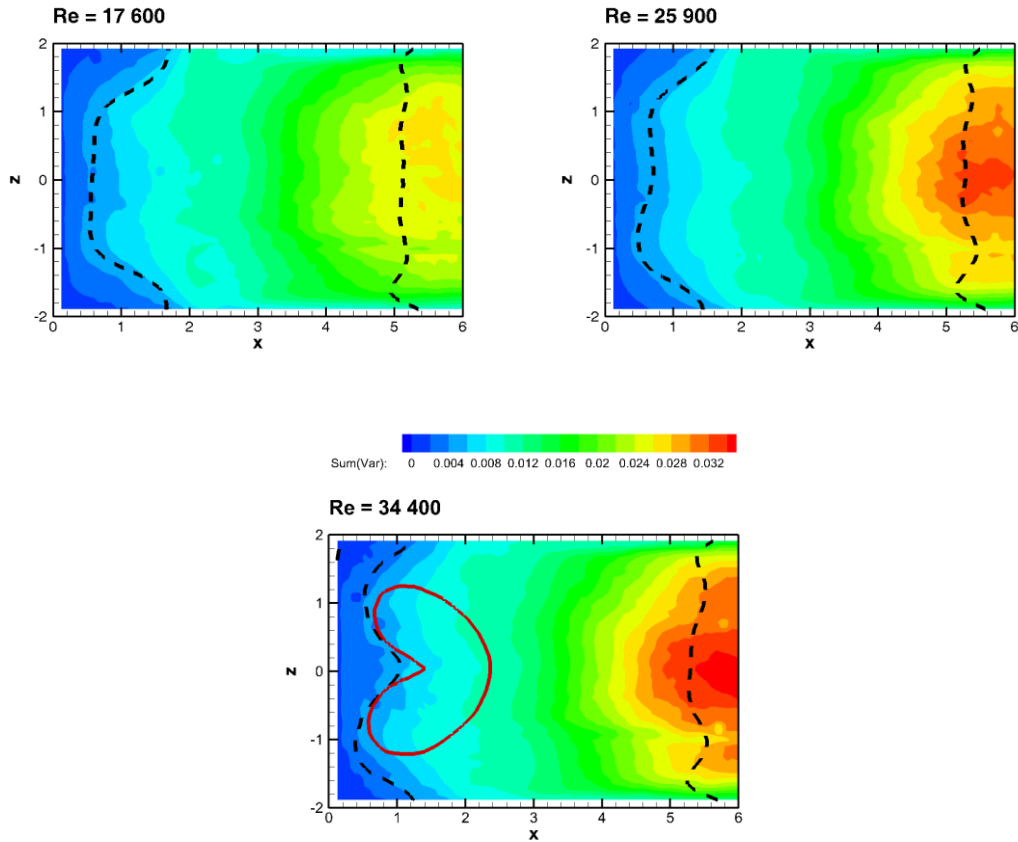


**Fig. 7** Sum of in-plane velocity components variation.  
 Reynolds numbers 7 200, 12 400, 17 600, 25 900 and 34 400.

The results show nearly no dynamical activity of the flow between the step and the line  $U = 0$ . Maximum fluctuating activity is located on the channel axis downstream the line of reattachment. The value of maximal variance is growing with the Reynolds number considerably from 0.025 up to 0.035, however the global maximum is located further downstream out of our frame. Note, that within the kidney region the fluctuating activity is moderate with values about 0.01. The kidneys upstream edge is bordered by the “no activity” region close to the step. This region is connected with the tertiary vortex next to the step root (compare Fig. 6), which seems to be relatively stable with weak dynamics.

## Conclusions

The time-mean topology of the flow behind backward-facing step in a narrow channel is studied in two sections for Reynolds numbers in range from 7 200 up to 34 400. Mean velocity fields and velocity variances distributions are presented.

The topology of the flow within the recirculation zone is highly 3D, however the reattachment line is close to be 2D. The secondary and higher order structures have been detected in the recirculation zone behind the step. The topology is of 3D nature and it is Reynolds number dependent. Stability of structures topology is better for higher Reynolds number.

The kidney structure on the channel bottom observed in previous studies has been explained only partially. Its upstream edge is connected with the stable tertiary vortex next to the step root.

Instantaneous structure of the recirculation zone is much more complex and will be addressed in follow-up studies dealing with the flow dynamics.

## Acknowledgements

This work was supported by the Grant Agency of the Czech Republic, project No. P101/10/1230.

## References

- [1] Bradshaw, P. *Variation on the Theme of Prandtl*, I.C.AeroRep., 1971, pp.71–73.
- [2] Uruba, V., *Mean structure of the flow over backward facing step in a narrow channel*. 31. Setkání kateder mechaniky tekutin a termomechaniky, Brno, Vysoké učení technické v Brně, 2012, (Jedelský, J.; Klimeš, L.), 2012, pp. 237-240.
- [3] Uruba, V., *Dynamics of flow behind backward-facing step in a narrow channel*. Experimental Fluid Mechanics 2012. Liberec : Technical University of Liberec, 2012, (Vít, T.; Dančová, P.; Novotný, P.), pp. 746-753.
- [4] Uruba, V., Jonáš, P. *Flow over back-facing step in a narrow channel*, Proceedings in Applied Mathematics and Mechanics. vol. 12, no. 1, 2012, pp. 501-502.
- [5] Uruba, V., *On structure of recirculation zone behind backward-facing step in a narrow channel*. Colloquium FLUID DYNAMICS 2012. Praha, Ústav termomechaniky AV ČR, v. v. i., 2012 (Jonáš, P.; Uruba, V.), pp. 33-34.
- [6] Uruba, V., Jonáš, P., Mazur, O., *Control of a channel-flow behind a backward-facing step by suction/blowing*, International Journal of Heat and Fluid Flow, Volume 28, Issue 4, August 2007, pp. 665–672.
- [7] Uruba, V., *Decomposition Methods in Turbulence Research*. EPJ Web of Conferences, Cedex A: EDP Sciences, 2012, (Wang, A.), 01095, pp. 24-44.
- [8] Uruba, V., *Dynamics of the Flow just behind Backward-Facing Step in Narrow Channel*. SKMTaT 2013, 25-28 June 2013, University of Žilina, pp. 287-290.